Nucleation Study on Deposition of Aluminum from 1-Butyl-3-Methylimidazolium Chloride and Aluminum Chloride Ionic Liquid Electrolyte

ECS Transactions, 98 (10) 199-208 (2020)
10.1149/09810.0199ecst ©The Electrochemical Society

Nucleation Study on Deposition of Aluminum from 1-butyl-3-methylimidazolium chloride (BMIC) and Aluminum chloride ($AlCl_3$) Ionic Liquid Electrolyte

Yuxiang Peng, Pravin. S. Shinde, and Ramana G. Reddy
Department of Metallurgical and Materials Engineering
The University of Alabama, Tuscaloosa, AL 35487, USA
Corresponding author: rreddy@eng.ua.edu; Tel: 205-348-4246

The aluminum is electrodeposited from an ionic liquid comprising a eutectic mixture of 1-butyl-3-methylimidazolium chloride (BMIC) and aluminum chloride ($AlCl_3$) at the $AlCl_3$ mole fraction of 0.667 (molar ratio of 1:2). The electrochemical behavior of chloroaluminate species in the ionic liquid (IL) is investigated by the chronoamperometry (CA) technique at different temperatures. The diffusion coefficients (D) of $Al_2Cl_7^-$ anion species in BMIC-$AlCl_3$ IL are calculated at various temperatures based on the chronoamperometric method. The calculated number densities of nucleation of Al deposits are 0.7×10^{10}, 1.0×10^{10}, and 1.4×10^{10} m^{-2} at 363 K with the applied potentials of −1.7, −1.75, and −1.8 V versus Pt, respectively. The scanning electron microscopy (SEM) result indicated that the calculated data is comparable to the experimental electrodeposition data. In addition, the rate of nucleation was also investigated during the electrodeposition experiment.

1. Introduction

In recent years, the room-temperature ionic liquid (IL) has been investigated as the electrolyte in the field of electrodeposition of metals or alloys (1). The IL is eco-friendly and efficient electrolyte due to its non-corrosive property, the wide temperature range for the liquid phase, the excellent thermal stability, low vapor pressure, wide electrochemical window, and low pollutant emission (2-4). In addition, they have recently been used as the electrolyte to reduce the Al element (2,5-8). However, the conventional processes of reducing Al require high temperatures that not only consume lots of energy but also release the unwanted greenhouse gases (9). Several ILs have been used to electrodeposit Al, which are synthesized by the combination of $AlCl_3$ with alkyl imidazolium chlorides (10-14). In fact, to understand the electrosythesis conditions and electrochemistry of this kind of ionic liquid, several properties have been reported in our group, such as the heat capacity (15), thermal stability (16,17), density (18), viscosity (18,19), thermodynamic (20-22), and electroanalytical (23-26) properties. One of the interesting ILs is BMIC-$AlCl_3$, which is liquid at room temperature. The mixture of the melt leads to the formation of several chloroaluminate anions, which exist in equilibrium, according to the following reactions (1-3) (10,11).

$$AlCl_3 + Cl^- \overset{room\ temperature}{\Longleftrightarrow} AlCl_4^- \quad [1]$$

$$AlCl_3 + AlCl_4^- \overset{room\ temperature}{\Longleftrightarrow} Al_2Cl_7^- \quad [2]$$

$$AlCl_3 + Al_2Cl_7^- \overset{room\ temperature}{\Longleftrightarrow} Al_3Cl_{10}^- \quad [3]$$

The amount of $AlCl_3$ determines the Lewis acidity of the BMIC-$AlCl_3$ melt. When the molar ratio of $AlCl_3$ and BMIC is less than 1, the melt consists of organic cation and tetra-chloroaluminate ions ($AlCl_4^-$). In the melts containing excess amount of $AlCl_3$ (molar ratio > 1), the excess $AlCl_3$ reacts with $AlCl_4^-$ anions to form Lewis acidic hepta-chloroaluminate ions ($Al_2Cl_7^-$) (27).

The electrochemical process of reduction of Al-species in the ILs is necessary to discuss before the utilization of ILs as the electrolyte. In fact, it has been illustrated previously that the electrodeposition process is due to the diffusion of $Al_2Cl_7^-$ species (2,14,28). And the nucleation of aluminum from BMIC-$AlCl_3$ IL follows the instantaneous process (2,29). However, the nucleation number densities at different conditions are still unclear in such IL. Even a few research studies illustrate the calculated and experimental nucleation number density in other ILs (1,30), the nucleation rate in the BMIC-$AlCl_3$ IL still unclear and needs to be investigated.

In this study, the melt of $AlCl_3$ with BMIC is employed for the nucleation study of the Al electrodeposition process. The CA experiments are performed to analyze the mechanism of diffusion and nucleation of aluminum-species from BMIC-$AlCl_3$ IL. Besides, Samples after electrodeposition were analyzed by Scanning Electron Microscope (SEM) and Energy Dispersive X-Ray Spectroscopy (EDS).

2. Experimental

The chemicals such as $AlCl_3$ (95%, Alfa-Aesar) and BMIC (98%, Sigma-Aldrich, HPLC grade) single salts were purchased and used as received. In the present work, the BMIC to $AlCl_3$ molar ratio of 1:2 was used to maximize the concentration of $Al_2Cl_7^-$ anion species in the ILs. Before the mixing process, the BMIC was placed in a vacuum oven to dry for at least 6 hours. Then, the chemicals were weighed in an appropriate ratio in a glove box under dry ultra-high purity (UHP, 99.995%) argon (Ar) gas. The BMIC was taken in a 250 mL beaker, and then $AlCl_3$ was slowly added into it at room temperature. A glass rod was used to stir while adding the $AlCl_3$. When the IL becomes a clear solution, it is transferred to another 50 mL beaker outside the glove box. The 50 mL beaker is covered by parafilm and placed on a hot plate and stirred for about 30 min for homogeneous mixing using a magnetic stirrer at 60 RPM. The temperature of the preheated hot plate was set to the experimental temperature (353 K).

The electrochemical experiments were performed with an EG&G PARC model 273 A potentiostat/galvanostat instrument controlled by Power Suite software. The CA curves were obtained by varying the overpotentials. The experiments were performed from BMIC-$AlCl_3$ IL using a three-electrode cell configuration. And each experiment was repeated at least two times to ensure repeatability. Figure 1 shows the schematic of the CA experimental setup.

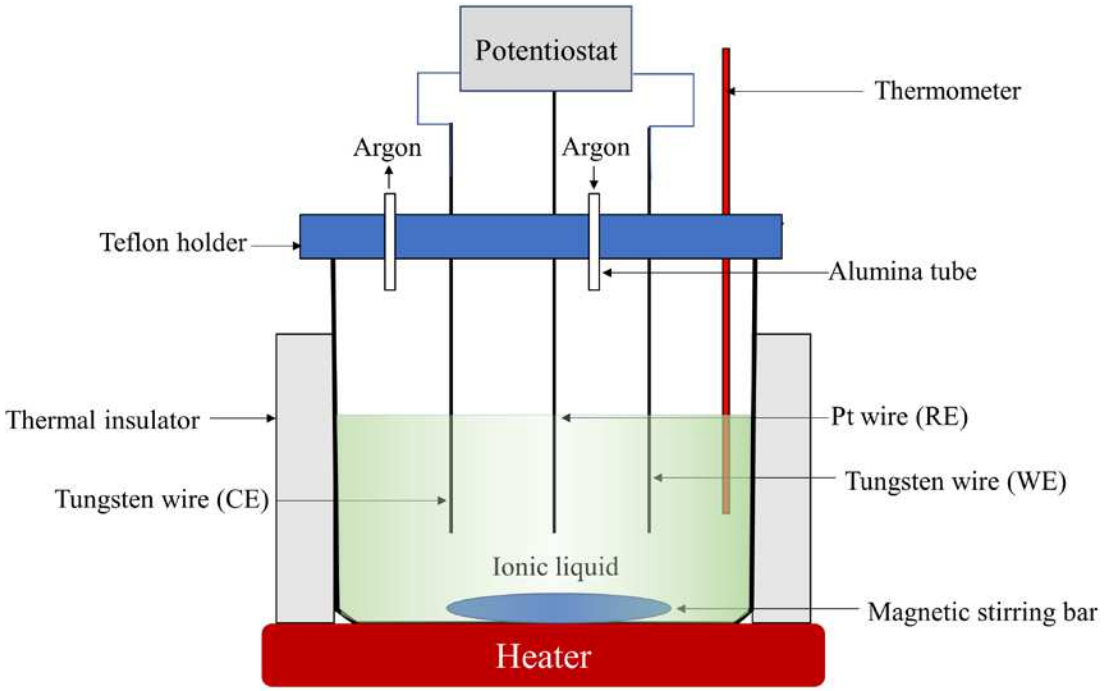

Figure 1. Schematic of an electrochemical cell for CA experiments in IL.

As shown in Figure 1, the temperature was controlled by a hot plate and was precisely monitored by the inserted thermometer. Tungsten wires (99.9%) with a diameter of 0.45 mm were used as working and counter electrodes, and the quasi-reference electrode was Pt wire (99.9%) with a 0.5 mm diameter. The Ar gas flow was continuously maintained through the alumina tube during the experiment. Thus, the whole system was under the Ar gas atmosphere. For the electrodeposition experiment, the experimental setup was similar to the CA experiment. But the working electrode was a Ni plate, and the counter electrode was an aluminum sheet. All the electrodes were ground with 800-grit SiC abrasive paper, washed with acetone and deionized water, and then dried by air right before the experiment. The height of the electrode immersed into the IL was measured after the experiment for area normalization.

3. Results and Discussion

3.1. Chronoamperometry (CA)

The chronoamperometric current-time transients for the BMIC-$AlCl_3$ IL at different applied potentials and different temperatures are shown in Figure 2. The area of a tungsten working electrode immersed in the IL is 2.8×10^{-5} m^2, and the quasi-reference electrode is Pt.

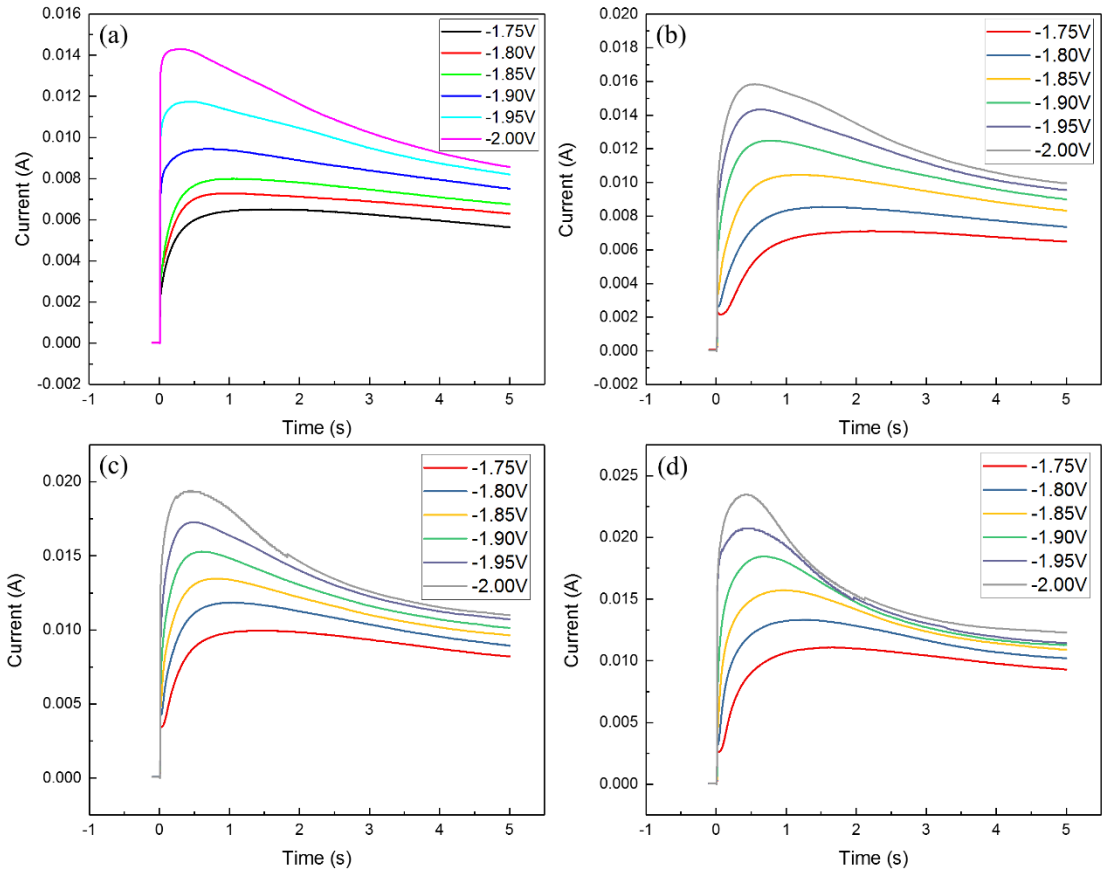

Figure 2. The chronoamperometric current-time transients for Al deposition from BMIC-$AlCl_3$ IL with different overpotentials at (a) 353 K, (b) 363 K, (c) 373 K, and (d) 383 K.

As shown in Figure 2, the applied overpotentials are sufficient to initiate the nucleation and growth of aluminum as the maximum current (I_m) and corresponding time (t_m) were observed. The current increased initially at a specific maximum value and then dropped. Moreover, when the applied overpotential is more negative, the value of the maximum current is increased while the corresponding time is decreased. As the cathodic potential increased, the nucleation rate and density of aluminum are increased (31).

3.2. Number density of nucleation and average radius

The dimensionless experimental current-time transients are compared with the dimensionless theoretically instantaneous and progressive nucleation model, which is described by Scharifker and Hills (32). The detailed expression is listed in equations [4-5], which present the relationship between dimensionless current density (j/j_m) to the dimensionless time (t/t_m).

$$Instantaneous: (j_{inst}/j_m)^2 = 1.9542(t_{inst}/t_m)^{-1}\{1 - exp[-1.2564(t_{inst}/t_m)]\}^2 \quad [4]$$

$$Progressive: (j_{prog}/j_m)^2 = 1.2254(t_{prog}/t_m)^{-1}\left\{1 - exp\left[-2.3367(t_{prog}/t_m)^2\right]\right\}^2 \quad [5]$$

where j is the current density (A m^{-2}) at any experimental time t, j_m is the maximum current density, and t_m time (s) is its corresponding time. The dimensionless current-time

transients for different potentials in BMIC-$AlCl_3$ IL along with theoretical nucleation processes are compared, as shown in Figure 3.

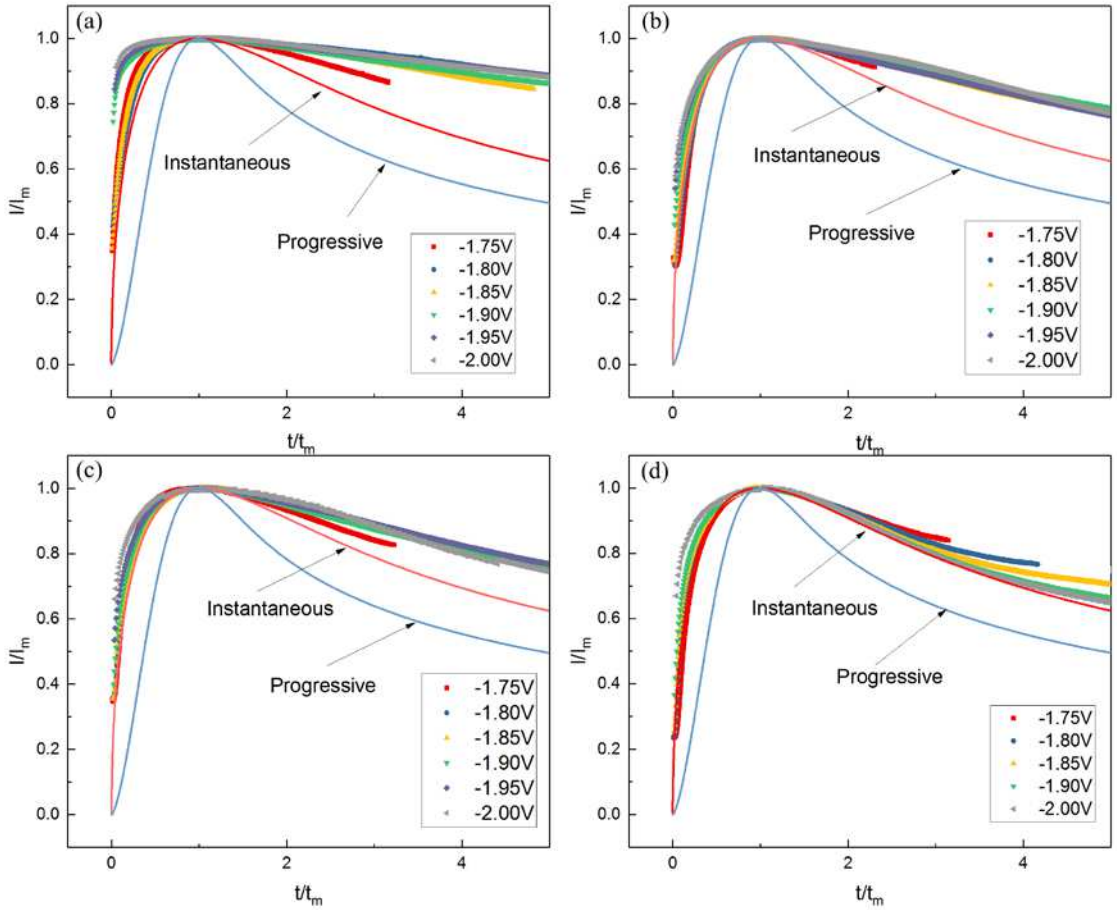

Figure 3. Comparison between experimental current-time transients at different potentials, in BMIC-$AlCl_3$ IL and theoretical instantaneous and progressive nucleation at (a) 353 K, (b) 363 K, (c) 373 K, and (d) 383 K.

As shown in Figure 3, the experimental results are closely relatable to the instantaneous nucleation process. At longer times, the experimental currents are larger than the theoretical values from the instantaneous nucleation model, reportedly due to partial kinetic control of the growth process (24,31).

As the electrodeposition of Al in BMIC-$AlCl_3$ IL follows three-dimension instantaneous nucleation and diffusion-control process, the number density of nucleation at different overpotentials can be calculated based on the model developed by Gunawardena *et al*. (33). The relation is given by equations [6-8].

$$j_m = 0.6382nFCD(kN)^{0.5} \quad [6]$$

$$j_m^2 t_m = 0.1629(nFC)^2 D \quad [7]$$

$$\mathrm{k} = (8\pi CM/\rho)^{0.5} \quad [8]$$

where the values of j_m and t_m are obtained from Figure 2, n is transferred electrons (0.75 mole for 1 mole $Al_2Cl_7^-$ diffusion), F is Faraday constant (96485C mol^{-1}), C is the concentration of $Al_2Cl_7^-$ (mol L^{-1}), D is diffusion coefficient (m^2 s^{-1}), k is a numerical constant, M is the atomic weight of aluminum (26.98 g mol^{-1}), ρ is the density of metallic aluminum (2700 g m^{-3}), and N is nucleation number density.

Based on the distribution of Al species in IL using the thermodynamic calculations (27) and the literature density data (34), the concentration of $Al_2Cl_7^-$ is calculated, which is listed in TABLE I.

TABLE I. Densities of BMIC-$AlCl_3$ IL and concentration of $Al_2Cl_7^-$ in the IL

Temperature (K)	Density × 10^6 (g m^{-3})	Concentration of $Al_2Cl_7^-$ (mol L^{-1})
353	1.29	2.34
363	1.28	2.32
373	1.27	2.30
383	1.26	2.28

Thus the average radius can be calculated based on the number density of nucleation (35) using equation [9].

$$r = (1/\pi N)^{0.5} \quad [9]$$

where r is the average radius (m), and N is the number density of nucleation (m^{-2}). And the calculated number density of nucleation at 363 K at different overpotentials is listed in TABLE II.

TABLE II. The calculated number density of nucleation (N) and the average radius (r) of the deposition of Al in BMIC-$AlCl_3$ at 363 K.

Potential (V) vs. Pt	N (m^{-2})	r (m)
-1.70	0.7×10^{10}	6.74×10^{-6}
-1.75	1.0×10^{10}	5.64×10^{-6}
-1.80	1.4×10^{10}	4.77×10^{-6}

As shown in TABLE II, the number density of nucleation is increased, while the average radius of deposition is decreased as the potential becomes more negative. To determine the influence of potential on the morphology of Al deposits, the electrodeposition experiments were performed on Ni plate at 363 K and different potentials (-1.7, -1.75, and -1.8 V vs. Pt). The working electrode and counter electrode used were Ni and Al plate in this experiment. The result is shown in Figure 4.

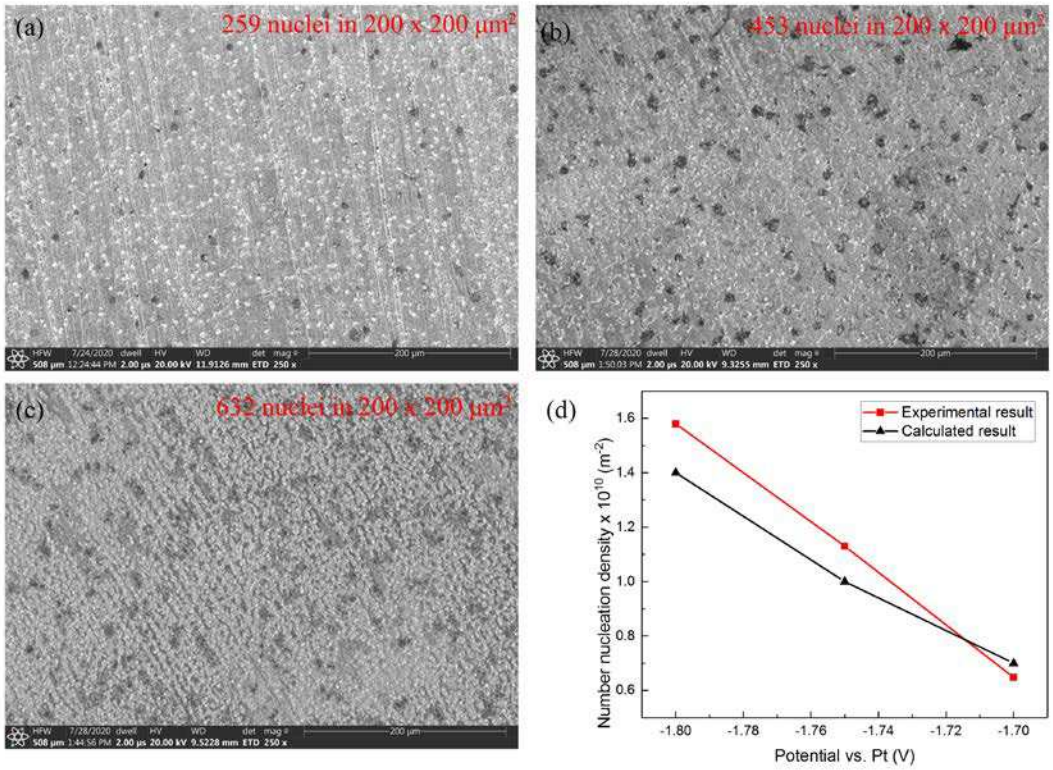

Figure 4. SEM micrographs of Al deposition on Ni substrates obtained in BMIC-$AlCl_3$ (1:2) IL for 1 min at 363 K and different potentials ((a) -1.7 V, (b) -1.75 V, and (c) -1.8 V) as well as (d) comparison of number nucleation density between experimental and calculated result.

As shown in Figure 4, the sphere depositions of Al are found on the Ni substrates at different constant potentials. In addition, the deposition is denser at a more negative potential. The number density of nucleation is counted in the 200 × 200 μm^2 area in the SEM micrographs and then calculated in 1 m^2 area. As shown in Figure 4(d), the calculated data (TABLE II) is comparable to the experimental result. The small difference may due to the formation of an exclusion zone in the model calculation (2).

The electrodeposition experiments were performed for different durations at -1.7 V vs. Pt at 363 K to investigate the growth rate of nucleation. And the result is shown in Figure 5.

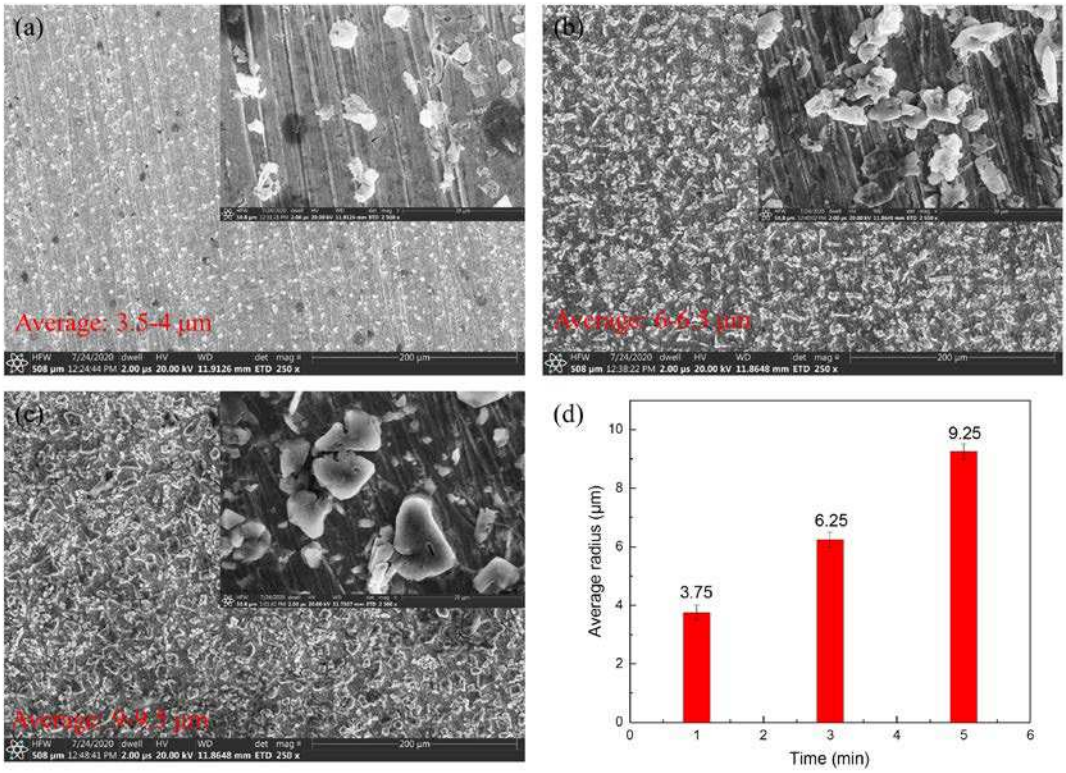

Figure 5. SEM micrographs of Al deposition on Ni substrates obtained in BMIC-$AlCl_3$ (1:2) IL at -1.7 V vs. Pt and 363 K for different time ((a) 1 min, (b) 3 min, and (c) 5 min); (d) a plot of the average radius of nucleation against time.

As shown in Figure 5, the average radius of the nucleation increases at a longer time and reaches to 9.25 μm for 5 min deposition. In addition, the growth rate is decreased for a long duration as the deposition becomes denser. The calculated average radius is 6.74 μm, as listed in TABLE II, which is slightly different from the experimental data. The little difference is due to the spherical grain assumed in the model calculation. In the real experiment, the deposition of nuclei growth is not spherical.

4. Conclusions

The nucleation process of Al electrodeposition in BMIC-$AlCl_3$ (1:2) is successfully evaluated by chronoamperometry in present work at different temperatures and different overpotentials. The result showed that deposition of Al involved in a three-dimension instantaneous nucleation process. In addition, the number density of nucleation is calculated at different applied potentials at 363 K based on the known concentration and diffusion coefficient of $Al_2Cl_7^-$ species. The morphological studies indicated that the deposition becomes denser at a more negative potential. And the number densities of nucleation are comparable between calculated and experimental results. Moreover, the growth rate of Al deposition is also studied in present work. It is found that the growth rate decreased for longer-time depositions. The calculated average nucleation radius is in a good agreement with experimental data.

Acknowledgments

The authors acknowledge the financial support received from the National Science Foundation (NSF) award number 1762522, Department of Energy (DOE) RAPID Manufacturing Institute and ACIPCO for this research project. Authors also thank the Department of Metallurgical and Materials Engineering, the University of Alabama for providing experimental and analytical facilities.

References

1. T. Jiang, M.C. Brym, G. Dubé, A. Lasia, G. Brisard, S*urf. Coat. Technol*. **201**(1-2) (2006) 10-18.
2. D. Pradhan, R.G. Reddy, *Mater. Chem. Phys.* **143**(2) (2014) 564-569.
3. R.G. Reddy, *J. Phase Equilib. Diff.* **27**(3) (2006) 210.
4. H. Yang, R.G. Reddy, *Electrochim. Acta* **178** (2015) 617-623.
5. R.T. Carlin, P.C. Trulove, H.C. De Long, *J. Electrochem. Soc.* **143**(9) (1996) 2747-2758.
6. J. Robinson, R. Osteryoung, *J. Electrochem. Soc.* **127**(1) (1980) 122-128.
7. P. Lai, M. Skyllas-Kazacos, *J. Electroanal. Chem. Interf. Electrochem.* **248**(2) (1988) 431-440.
8. D. Pradhan, R. Reddy, *Electrochim. Acta* **54**(6) (2009) 1874-1880.
9. D. Pradhan, R.G. Reddy, *Metall. Mater. Tran. B* **43**(3) (2012) 519-531.
10. P. Koronaios, D. King, R.A., *Inorg. Chem.* **37**(8) (1998) 2028-2032.
11. V. Kamavaram, D. Mantha, R. Reddy, *Electrochim. Acta* **50**(16-17) (2005) 3286-3295.
12. Q. Liao, W.R. Pitner, G. Stewart, C.L. Hussey, G.R. Stafford, *J. Electrochem. Soc.* **144**(3) (1997) 936.
13. Y. Zhao, T. VanderNoot, *Electrochim. Acta* **42**(11) (1997) 1639-1643.
14. T. Jiang, M.C. Brym, G. Dubé, A. Lasia, G. Brisard, *Surf. Coat. Technol.* **201**(1-2) (2006) 1-9.
15. J.D. Holbrey, W.M. Reichert, R.G. Reddy, R.D. Rogers, ACS Publications **856**(11) (2003) 121-133.
16. V. Kamavaram, R.G. Reddy, *Int. J. Therm. Sci.* **47**(6) (2008) 773-777.
17. R.G. Reddy, Z. Zhang, M.F. Arenas, D.M. Blake, *High Temp. Mater. Proc.* (London) **22**(2) (2003) 87-94.
18. V. Karmavaram, R.G. Reddy, Aluminum 2003, S.K. Das Ed., TMS, (2003) 299-308.
19. V. Kamavaram, R. Reddy, Light Metals 2005, TMS, Warrendale, PA (2005) 501-05.
20. R. Reddy, A. Yahya, L. Brewer, *J. Alloy. Compd.* **321**(2) (2001) 223-227.
21. M. Zhang, V. Kamavaram, R.G. Reddy, *J. Phase Equilib. Diff.* **26**(2) (2005) 124-130.
22. M.M. Zhang, R.G. Reddy, *Min. Proc. Ext. Met.* **119**(2) (2010) 71-76.
23. A. Liu, Z. Shi, R.G. Reddy, *Ionics* **26**(6) (2020) 3161-3172.
24. A. Liu, Z. Shi, R.G. Reddy, *Electrochim. Acta* **251** (2017) 176-186.
25. A. Liu, Z. Shi, R.G. Reddy, *J. Electrochem. Soc.* **164**(9) (2017) D666-D673.
26. M. Li, Z. Wang, R.G. Reddy, *J. Electrochem. Soc*. **161**(4) (2014) D150-D153.
27. V. Kamavaram, D. Mantha, R. Reddy, *J. Min. Metall. B* **39**(1-2) (2003) 43-58.

28. J. Tang, K. Azumi, *Electrochim. Acta* **56**(3) (2011) 1130-1137.
29. Y. Zheng, C. Peng, Y. Zheng, D. Tian, Y. Zuo, Y. Zheng, *Int. J. Electrochem. Sci.* **11** (2016) 6095-6109.
30. J.J. Lee, B. Miller, X. Shi, R. Kalish, K.A. Wheeler, *J. Electrochem. Soc.* **147**(9) (2000) 3370-3376.
31. H. Yang, R.G. Reddy, *J. Electrochem. Soc.* **161**(10) (2014) D586-D592.
32. B. Scharifker, G. Hills, *Electrochim. Acta* **28**(7) (1983) 879-889.
33. G. Gunawardena, G. Hills, I. Montenegro, *Electrochim. Acta* **23**(8) (1978) 693-697.
34. V. Kamavaram, Novel electrochemical refining of aluminum based materials in low temperature ionic liquid electrolytes, Dissertation, The University of Alabama, 2004.
35. R.T. Carlin, W. Crawford, M. Bersch, J. *Electrochem. Soc.* **139**(10) (1992) 2720-2727.